Journal of Computational Physics **170,** 395–414 (2001)
doi:10.1006/jcph.2001.6741, available online at http://www.idealibrary.com on IDEAL®

High-Speed Switch-On of a Semiconductor Gas Discharge Image Converter Using Optimal Control Methods

J.-H. R. Kim,* H. Maurer,* Yu. A. Astrov,† M. Bode,† and H.-G. Purwins†

*Institut für Numerische Mathematik, WWU Münster, Einsteinstr. 62, D-48149 Münster, Germany; and †Institut für Angewandte Physik, WWU Münster, Corrensstr. 2/4, D-48149 Münster, Germany
E-mail: maurer@math.uni-muenster.de

Received October 25, 2000; revised January 17, 2001

Experiments evidence that optical commutation of current in semiconductor gas discharge devices from a low to a high value may be accompanied by an oscillatory mode of such a transient and by a long effective time for the transition. For a simple two-component model of transport processes in these nonlinear systems, which encounter the main observed features in dynamics, the problem of minimizing the time of switching on the high current state is considered. This problem can be formulated as an optimal control problem with control function provided by a proper temporal variation of the feeding voltage. It is shown that the optimal control can substantially shorten the effective transient time of the process and totally suppress the occurrence of an overshooting in a transient. Optimal control strategies for constraints on control and state variables and for different parameters are presented.

Key Words: imaging device; nonlinear electronic system; high-speed operation; optimal voltage control; minimal transient time; bang–bang control; time optimal control; Lotka–Volterra system.

1. INTRODUCTION

Optimal control methods for optimizing the behavior of dynamical systems have been used in a variety of fields of applied science [1–6]. To a large extent, the success of optimal control rests on the accurate modeling of the dynamical process via ordinary or partial differential equations. Although many processes in applied physics are adequately modeled by differential equations, a systematic application of optimal control methods may be rarely found. The purpose of this paper is to provide such an example in applied physics, namely, the optimal control of a semiconductor gas discharge image converter.

Many technical devices function in nonlinear regimes. Examples are lasers [7] and different semiconductor devices [8, 9]. Many applications, e.g., pulse lasers in technology and

0021–9991/01 $35.00

optical communication, require a stable and controllable operation of devices. Lippi *et al.* [10–12] have suggested a method for controlling gas discharge CO_2 and semiconductor lasers to suppress oscillations in the emitted power of transient modes and to shorten the time lag in a pulse. To reach these goals, they use a simplified dynamical model for the considered laser, namely, a two-component Lotka–Volterra system. During the past decades a large interest has been manifested in the study of electronic microdischarge devices [13–15]. Compared to high-power discharge systems (e.g., arc discharge devices), microdischarge devices are characterized by a small characteristic dimension of the discharge volume, by a low density of charge carriers in the discharge gap, and, as a consequence, by a relatively low electrical power dissipated in a device. Under these conditions, characteristic impedances of components of a device are rather high and influence its dynamics, particularly at varying control parameters. The peculiarities of the transient processes of gas discharge systems are also related to its nonlinear nature.

The nonlinearity of self-sustained gas discharges originates from the mechanism of current transport in a gas: it is related to the autocatalytic multiplication of charge carriers in the interelectrode space of a device with electric field E. Therefore, the efficiency of this process is to a large extent dependent on the amplitude of the field E [17]. In addition, such a mechanism has a pseudoinductive nature: the density N of carriers in the gap follows a variation in E with a time lag. The general feature of self-sustained gas discharges is that they cannot operate in a stable fashion without an external load. In the opposite case the current would grow indefinitely; evidently, this would destroy the device. Together with the natural capacitance of the discharge volume, such a load contributes to the capacitance of the whole device. Even in the stable operation of the device, the capacitance and the pseudoinductance can initiate the appearance of damped oscillations in transient processes.

In the present article, we consider the problem of optimal control of one of the simplest gas discharge systems, which is the semiconductor gas discharge device initially designed for the conversion of infrared (IR) images to the visible range of light [15, 18]. The feeding voltage is taken as the control function. The basic idea of our research is closely related to the work of Lippi *et al.* [10–12], in which steering schemes of a gas discharge pulse CO_2 laser which improve the transient time dramatically are developed. Although these control strategies are not derived on the basis of optimal control theory, they expose some characteristic features of optimal bang–bang controls.

Here, we deal with a different device and, therefore, with equations different from those in [10–12]. In the resulting optimal control model, we compute optimal control functions for a variety of parameters and constraints. It turns out that the optimal control is a bang–bang control exhibiting only two bang–bang arcs. The efficiency of optimal control strategies is demonstrated by the fact that one can substantially decrease the duration of transient processes and nearly totally suppress an overshooting in the output signal. The results obtained can be used in applications of semiconductor gas discharge devices, such as fast converters of infrared images [15, 18], and in the development of pulse sources of light, e.g., of ultraviolet excimer microdischarge lamps [13]. We indicate that the dynamical systems considered here and in [10–12] can be transformed into the same type of Lotka–Volterra system by an appropriate scaling of the state and time variables. Thus we may hope to apply the optimal control methods of the present paper also to the problems considered in [10–12]. This may eventually lead to a further refinement of results obtained in the cited papers.

2. THE DEVICE AND BASIC EQUATIONS

The device is presented schematically in Fig. 1. It consists of two main components: a semiconductor layer (A) and a gas discharge domain (B). The planar structure is fed by a voltage source U that is connected to plane electrodes (C) and (D), which are in contact with the semiconductor and gas discharge components, respectively.

Other conditions being equal, the current in the device is dependent on the resistance of the semiconductor electrode, which is a spatially distributed load for the discharge domain. The resistivity ρ of the electrode can be varied with the illumination from a source of infrared light. In this way, the system can operate as a converter of infrared images [15, 18]. To provide high spatial resolution, the device must have a rather small thickness of the discharge gap d that is typically on the order of 100 μm. At a moderate residual pressure of gas in the gap, the simplest (Townsend) mode of discharge is then observed in a broad range of current density (for the definition of the Townsend discharge see, e.g., [17]). The technical importance of the device has its origin in the fact that fast cameras which allow the acquisition of images do exist in the visible range but not in the infrared. With the above-mentioned converter the range of operation can be extended up to a wavelength on the order of 11 μm.

At fixed physical parameters (such as the gas pressure and thickness of both the semiconductor and the discharge gap), the steady-state value of electric current density is determined by ρ and the magnitude of U. The response of the system to an abrupt variation of these control parameters can be rather complicated; see Fig. 2, where an example of the transition to a new (increased) value of current and, correspondingly, to the increased intensity of the discharge glow is given. This transition is initiated by a step-like decrease of ρ resulting from a pulse irradiation of the semiconductor electrode by an IR laser. This transition is

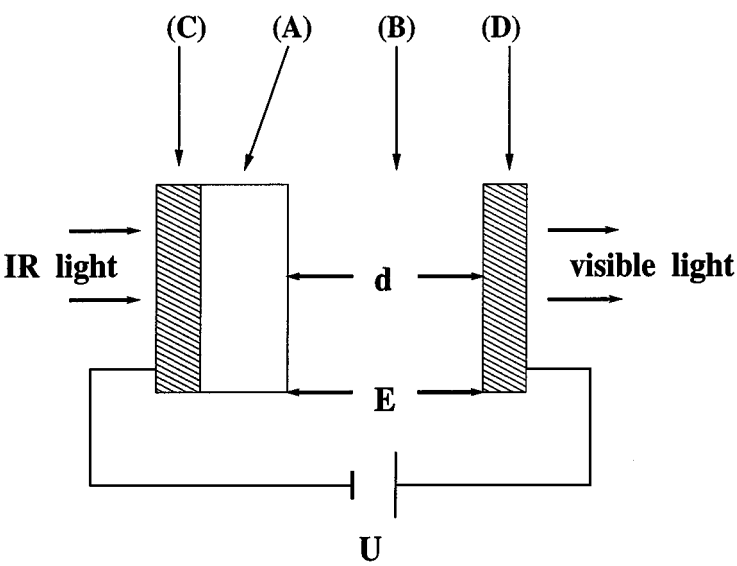

FIG. 1. Schematic presentation of the device. The layered structure consists of a semiconductor part (A) and a gas-filled gap (B). It is fed by a dc voltage U via transparent electrodes (C, D). When U exceeds some critical value U_c, a self-sustained discharge develops in the gap. The discharge emits the visible light. Its intensity is determined by the current in the device. The value of current can be controlled by the resistivity ρ of the semiconductor.

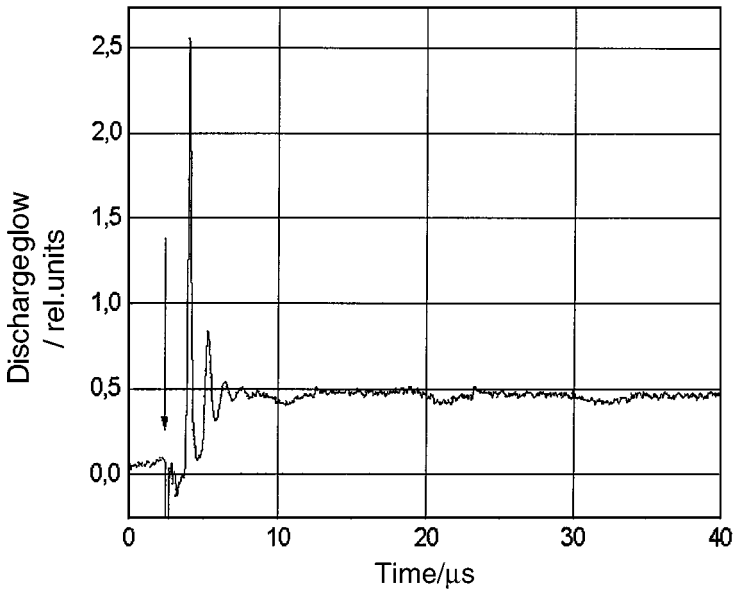

FIG. 2. A typical response of the device to the light excitation from an infrared step-like laser pulse which starts at time $t = t_0$ (as indicated by the arrow). The oscilloscopic trace shows the dynamics of the discharge glow, which has intensity proportional to the current. The negative spike in the signal at t_0 is due to the switching on the electrooptical modulator of the laser setup and is not related to the dynamics of the discharge glow.

due to the internal photo effect, and we will assume throughout the paper that the change of incoming radiation, as well as the accompanied change of ρ, is fast compared to all other relevant time constants of the system.

Two characteristic features are seen in the response of the system to the pulsed excitation: the existence of delay in increasing the current and the appearance of characteristic nonlinear oscillations in kinetics. These peculiarities are quite general for systems with nonlinear dynamics when the state is abruptly changed [10–12].

The main features in dynamical properties of the device can be described by the following two differential equations for the electric field $E(t)$ in the discharge gap at time $t \geq 0$ and the density $N(t)$ of the charge carriers; cf. [15, 16]:

$$\frac{dE}{dt} = \frac{E_M(t) - E(t)}{\tau_M} - bN(t)E(t), \tag{1}$$

$$\frac{dN}{dt} = \frac{N(t)}{\tau_r}\left(\frac{E(t)}{E_c} - 1\right). \tag{2}$$

All constants will be specified below. The quantity $E_M(t)$ is defined by

$$E_M(t) := \frac{U(t)}{d}, \tag{3}$$

where $U(t)$ denotes the amplitude of the feeding voltage. Its typical value used practically lies in the range 800–1000 V. Application of higher voltages may destroy the semiconductor layer because of its electrical breakdown. Therefore, in the present analysis the following

condition is imposed on the voltage:

$$0 \le U(t) \le 1\ [\mathrm{kV}]. \tag{4}$$

However, in Section 4.1, we will also study the case of higher voltages to clarify whether this could give an essential increase in the speed of the device compared to the control bounds (4).

The parameter τ_M is proportional to the resistivity ρ of the electrode [15, 16]. First, we will study the behavior of the dynamical system (1) and (2) for the time-independent function $U(t) \equiv 1\,\mathrm{kV} \ge E_c d$. A standard stability analysis reveals that the stationary point

$$\left(E_c, \frac{1}{b\tau_M}\left(\frac{E_M^0}{E_c} - 1\right)\right), \quad \text{where } E_M^0 := 1\ \mathrm{kV}/d \text{ in view of (3)}, \tag{5}$$

is asymptotically stable since the eigenvalues α_1 and α_2 of the Jacobian have negative real parts:

$$\mathrm{Re}(\alpha_i) = -2.5\frac{\tau_r}{\tau_M}, \quad i = 1, 2. \tag{6}$$

Before starting the process at $t = 0$, a fixed value $\tau_M = \tau_M^0$ is chosen. Hence, at $t = 0$ the system (1), (2) starts in the *stable* stationary point

$$E(0) = E_c, \qquad N(0) = N_0 := \frac{1}{b\tau_M^0}\left(\frac{E_M^0}{E_c} - 1\right). \tag{7}$$

From time $t = 0$ on, the system (1), (2) evolves with a smaller value $\tau_M < \tau_M^0$ which models an excitation. Then according to (5), the *stable* stationary point is given by

$$(E_c, N_f) \quad \text{with } N_f := \frac{1}{b\tau_M}\left(\frac{E_M^0}{E_c} - 1\right). \tag{8}$$

The subscript f in N_f refers to the final position to be considered quantitatively later. As a consequence of (6), the solution $(E(t), N(t))$ of(1), (2), using the time-independent voltage $U(t) \equiv 1$ kV, converges to the stationary point (8),

$$\lim_{t\to\infty} (E(t), N(t)) = (E_c, N_f).$$

This property is confirmed by the following simulation, which has been carried out for the parameters

$$\begin{aligned} &d = 100\ \mu\mathrm{m}, \qquad E_M^0 = 10^5\ \mathrm{V/cm}, \qquad E_c = 2 \times 10^4\ \mathrm{V/cm}, \\ &b = 5 \times 10^{-3}\ \mathrm{cm^3/s}, \qquad \tau_r = 10^{-7}\ \mathrm{s}, \qquad \tau_M^0 = 6.5 \times 10^{-3}\ \mathrm{s}, \end{aligned} \tag{9}$$

which are close to those characteristics for the description of the converter with an initial current of low density (for details see [15]). To model moderate excitations, the parameter τ_M is varied in the range 10^{-5} to 10^{-3} s. The dashed line in Fig. 3a shows the strong oscillatory behavior of $N(t)$, which is in qualitative agreement with the experimental results in Fig. 2. Let us denote by t_{10} the time when the deviation of the solution $(E(t), N(t))$ from the

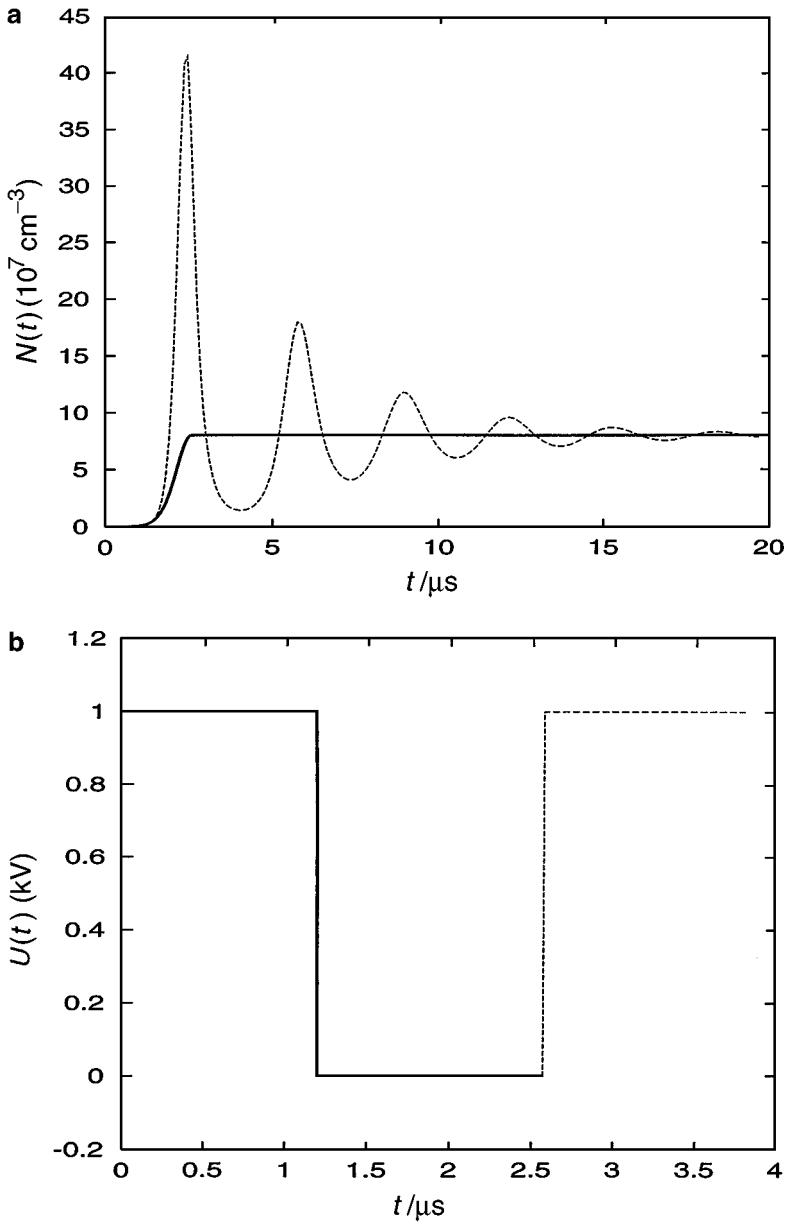

FIG. 3. $\tau_M = 10^{-5}$ s: (a) Carrier density $N(t)$ for $U(t) \equiv 1$ kV (dashed line) and for optimal control $U(t)$ (solid line). (b) Optimal control $U(t)$.

stationary point (E_c, N_f) in (8) is less than 10%. The values of t_{10} for different parameters τ_M are given in Table I.

To avoid strong oscillations of the free carriers, we can benefit from the key ideas of optimal control theory [1–3]. Instead of taking the feeding voltage as a time-constant value $U(t) \equiv 1$ kV, we consider it as a *time-dependent* control function $U(t)$ which is taken from the class of piecewise continuous functions. Making use of the additional degrees of freedom in the choice of the control $U(t)$, the system is able to reach the stationary point

(8) in a *finite* time $t_f > 0$; i.e., the solution satisfies

$$E(t_f) = E_c, \qquad N(t_f) = N_f. \tag{10}$$

This goal has also been achieved in [10–12] for equations similar to (1) and (2). Going a step further than the approach in [10–12], our objective is to minimize the time t_f for which (10) holds. It turns out that the optimized time is dramatically less than the time t_{10} representing the 10% deviation from the stationary points in the uncontrolled case. Moreover, the optimized transient time will have the favorable effect that all oscillations in transients are suppressed.

3. MINIMAL TRANSIENT TIME BY OPTIMAL CONTROL METHODS

In this section, we study the following optimal control problem: determine a piecewise continuous optimal control function $U : [0, t_f] \to [0, 1]$ and a minimal final time t_f such that the solution $(E(t), N(t))$ of Eqs. (1) and (2) satisfies the initial and final conditions (7) and (10). An optimal solution of this problem is characterized by first-order optimality conditions in the form of a *minimum principle* [1–3]. These conditions are formulated with the help of the *Hamilton function* that has the following form in our problem:

$$\begin{aligned} H(E, N, \lambda_E, \lambda_N, U) &= \lambda_0 + \lambda_E \frac{dE}{dt} + \lambda_N \frac{dN}{dt} \\ &= \lambda_0 + \lambda_E \left(\frac{U/d - E}{\tau_M} - bNE \right) + \lambda_N \frac{N}{\tau_r} \left(\frac{E}{E_c} - 1 \right). \end{aligned} \tag{11}$$

The scalar variables λ_E, λ_N are called *adjoint variables* while λ_0 is a scalar satisfying $\lambda_0 \geq 0$. Let $U(t)$ be the optimal control, $(E(t), N(t))$ the optimal trajectory, and t_f the minimal final time. Then there exist continuous and piecewise differentiable functions $\lambda_E; \lambda_N : [0, t_f] \to \mathbb{R}$ with $(\lambda_0, \lambda_E(t), \lambda_N(t)) \neq 0, \lambda_0 \geq 0$ for all $t \in [0, t_f]$ such that the following three conditions hold for almost all $t \in [0, t_f]$:

1. *Adjoint equations*

$$\begin{aligned} \frac{d}{dt}\lambda_E(t) &= -\frac{\partial}{\partial E} H(E(t), N(t), \lambda_E(t), \lambda_N(t), U(t)) \\ &= \frac{\lambda_E(t)}{\tau_M} + b\lambda_E(t)N(t) - \frac{\lambda_N(t)N(t)}{\tau_r E_c}, \end{aligned} \tag{12}$$

$$\begin{aligned} \frac{d}{dt}\lambda_N(t) &= -\frac{\partial}{\partial N} H(E(t), N(t), \lambda_E(t), \lambda_N(t), U(t)) \\ &= b\lambda_E(t)E(t) - \frac{\lambda_N(t)}{\tau_r} \left(\frac{E(t)}{E_c} - 1 \right). \end{aligned} \tag{13}$$

2. *Minimum condition for the optimal control*

$$H(E(t), N(t), \lambda_E(t), \lambda_N(t), U(t)) = \min_{U \in [0,1]} H(E(t), N(t), \lambda_E(t), \lambda_N(t), U). \tag{14}$$

3. *Transversality condition for the autonomous system*

$$H(E(t), N(t), \lambda_E(t), \lambda_N(t), U(t)) \equiv 0. \tag{15}$$

Note that variable U on the right side of (14) plays the role of a formal variable. Because the control variable U enters *linearly* into the Hamilton function, the minimum condition (14) simplifies to the minimization problem

$$\sigma(t) \cdot U(t) = \min\{\sigma(t) \cdot U \mid U \in [0, 1]\} \qquad \text{for all } t \in [0, t_f], \tag{16}$$

where the so-called *switching function* $\sigma(t)$ is given by

$$\sigma(t) := \frac{\partial}{\partial U} H(E(t), N(t), \lambda_E(t), \lambda_N(t), U(t)) = \frac{\lambda_E(t)}{\tau_M d}. \tag{17}$$

Because $\tau_M d > 0$, the minimum condition (16) immediately leads to the following characterization of the optimal control:

$$U(t) = \begin{cases} 0, & \text{if } \lambda_E(t) > 0, \\ 1, & \text{if } \lambda_E(t) < 0, \\ \text{singular}, & \text{if } \lambda_E(t) \equiv 0 \quad \forall t \in J := [t_a, t_b] \subset [0, t_f]. \end{cases} \tag{18}$$

This condition means that the optimal control $U(t)$ can be a combination of *bang–bang arcs*, where $U(t) \in \{0, 1\}$ and $\lambda_E(t) \neq 0$ holds, and *singular arcs* with $\lambda_E(t) \equiv 0 \, \forall t \in J = [t_a, t_b] \subset [0, t_f]$. First, we exclude the case of a singular control. Suppose that $\lambda_E(t)$ vanishes on a singular arc. Then the adjoint equation (12) yields the relation

$$0 \equiv \frac{d}{dt}\lambda_E(t) = \frac{\lambda_E(t)}{\tau_M} + b\lambda_E(t)N(t) - \frac{\lambda_N(t)N(t)}{\tau_r E_c} = \frac{\lambda_N(t)N(t)}{\tau_r E_c}.$$

In this equation we can eliminate the case $N(t) = 0$, since $N(t_0) = 0$ for one point $t_0 \in [t_a, t_b]$ would entail $N(t) \equiv 0$ for all $t \geq t_0$. Hence, the last equation yields $\lambda_N(t) \equiv 0$, which results in $\lambda_0 = 0$ in view of the definition of the Hamilton function (11) and the transversality condition (15). But the vanishing of all multipliers contradicts the statement $(\lambda_0, \lambda_E(t), \lambda_N(t)) \neq 0 \, \forall t \in [0, t_f]$ in the minimum principle. Hence, singular arcs cannot occur as part of the optimal control.

Thus we have shown that the switching function $\sigma(t)$, respectively $\lambda_E(t)$, has only isolated zeroes and that the optimal control is bang–bang. The optimal control can only switch from the value 0 to 1 or vice versa at the zeroes of the switching function, which are called *switching points*. The numerical task now consists in determining the number of bang–bang arcs and the exact location of the switching points. Observe that the control law (18) does not give any further information on the number of bang–bang arcs. To prepare the computation of the optimal control, we shall assume the control structure

$$U(t) = \begin{cases} 1, & \text{if } 1 \leq t < t_1, \\ 0, & \text{if } t_1 \leq t < t_f. \end{cases} \tag{19}$$

Essentially, there are two numerical methods for computing the optimal solution and verifying the structure (21). Several authors have developed nonlinear optimization techniques for solving a discretized version of the control problem. This approach has been implemented, e.g., in the efficient code NUDOCCCS of [20]. To sketch the other method, we observe that the optimal solution satisfies a *boundary-value problem* (BVP) which is composed of the

state equations (1), (2), (7), (10), the adjoint equations (12), (13), and conditions (15), (16). This type of a BVP can be conveniently solved by *shooting methods* as implemented in the code BNDSCO of [22].

The second method can be applied in the following way. First, one applies a Newton method to compute the precise values of the switching point t_1 and the minimal final time t_f. These values are implicitly determined by the two terminal state conditions $E(t_f) = E_c$ and $N(t_f) = N_f$ upon using the control law (19). For the parameter $\tau_M = 10^{-5}$ s we obtain

$$t_1 = 1.18806354\ \mu\text{s}, \quad t_f = 2.56577562\ \mu\text{s}.$$

The time t_1, respectively t_f, is given here with high precision only for the sake of demonstrating the accuracy of the mathematical method. From a technical point of view it suffices to round off to two decimal places; i.e., we have $t_1 = 1.19\ \mu s$ and $t_f = 2.57 \mu s$.

To compute the adjoint variables $\lambda_E(t), \lambda_N(t)$ we may set the multiplier $\lambda_0 = 1$ in the Hamilton function (11). In the numerical analysis of control problems, it is common practice to assume this *normal* form of the optimality conditions. Using the transversality condition (15), we see that the initial value $\lambda_E(0)$ is given by

$$\lambda_E(0) = -\frac{\tau_M \tau_M^0}{\left(E_M^0 - E_c\right)\left(\tau_M^0 - \tau_M\right)}. \tag{20}$$

The final step is to compute the initial value $\lambda_N(0)$. This value is implicitly determined by the switching condition $\lambda_E(t_1) = 0$, when integrating the adjoint equations (12) and (13) with the initial condition (20) and the unknown value $\lambda_N(0)$. This procedure gives the following numerical results:

$$\tau_M = 10^{-5}\,\text{s}: \qquad \lambda_E(0) = -1.25192600 \times 10^{-10}, \quad \lambda_N(0) = -18.0900162 \times 10^{-13}.$$

Figure 3 displays the optimal density $N(t)$ of carriers and the optimal control $U(t)$. The dashed part of the optimal control refers to the fact that the constant voltage $U(t) \equiv 1\,\text{kV}$, $t \geq t_f = 2.57\ \mu\text{s}$, is applied to keep the system at the stationary point (dashed continuation of the trajectories in Fig. 4).

The optimal density of carriers in Fig. 3 is contrasted with the uncontrolled density of carriers using the constant voltage $U(t) \equiv 1\,\text{kV}$. The data clearly demonstrate the capability of the control procedure to suppress any oscillations in the transient process. This fact is further illustrated in Fig. 4, which depicts the the electric field and the carrier density in greater detail. The optimal adjoint variables are shown in Fig. 5, where it is indicated that the control laws (18) and (19) are satisfied. The optimal bang–bang control strategy in Fig. 3 exhibits a strong similarity with control schemes proposed in [10–12] for steering laser transients. This comes as no surprise since the Lotka–Volterra system (1) and (2) has the same mathematical structure as the one considered in [10–12]. We shall discuss this subject in more detail in the next section. The problem of control was not analyzed on the basis of optimal control theory in [10–12]. We may hope therefore to validate or refine these results by optimal control methods similar to those developed in the present paper.

Figure 6 shows similar control strategy and behavior of the optimal density of carriers for $\tau_M = 10^{-4}$ s. Table I summarizes the results for different values of τ_M. Recall that the

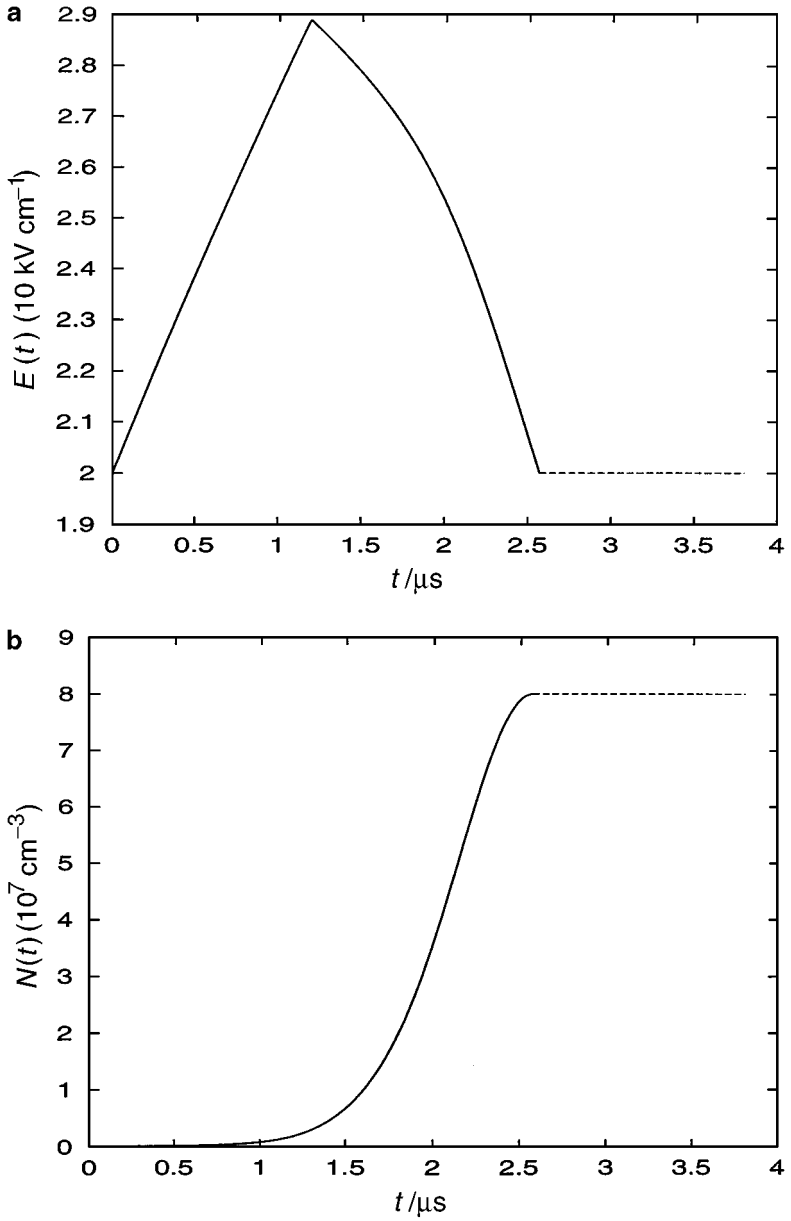

FIG. 4. Optimal solution $E(t)$ and $N(t)$ for $\tau_M = 10^{-5}$ s.

notation t_{10} refers to the time at which the uncontrolled system with $U(t) \equiv 1$ kV reaches the final stationary point within 10% accuracy. A dramatic improvement in transient times is observed to be more distinct with increasing parameter value τ_M.

The switching point t_1 has to be applied to the system with high accuracy to avoid further oscillations. However, even for a deviation of the parameter τ_M within 10% of the chosen parameter τ_M, one still observes a clear improvement compared to the uncontrolled device. This property is illustrated in Fig. 7, where transient times t_{10} for different control functions are given and the corresponding carrier densities $N(t)$ are compared.

TABLE I

Optimal Switching Time t_1 and Final Time t_f in Comparison with t_{10} Where the Uncontrolled System with $U(t) \equiv 1$ kV Reaches the Final Stationary Point within 10% Accuracy

τ_M	t_1	t_f	t_{10}
10^{-5} s	1.19 μs	2.57 μs	14 μs
5×10^{-5} s	2.25 μs	4.98 μs	67 μs
10^{-4} s	3.01 μs	6.51 μs	130 μs
5×10^{-4} s	5.99 μs	11.42 μs	650 μs
10^{-3} s	8.14 μs	14.08 μs	$>$1000 μs

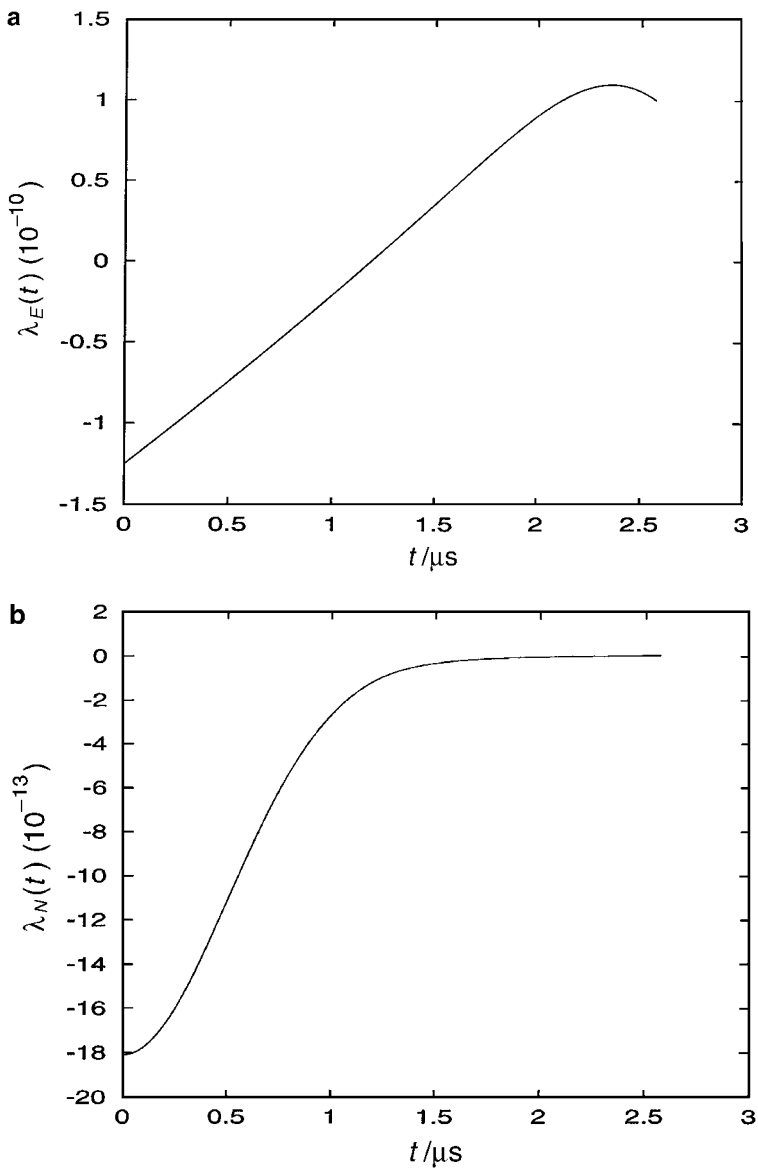

FIG. 5. Adjoint variables $\lambda_E(t)$ and $\lambda_N(t)$ for $\tau_M = 10^{-5}$ s.

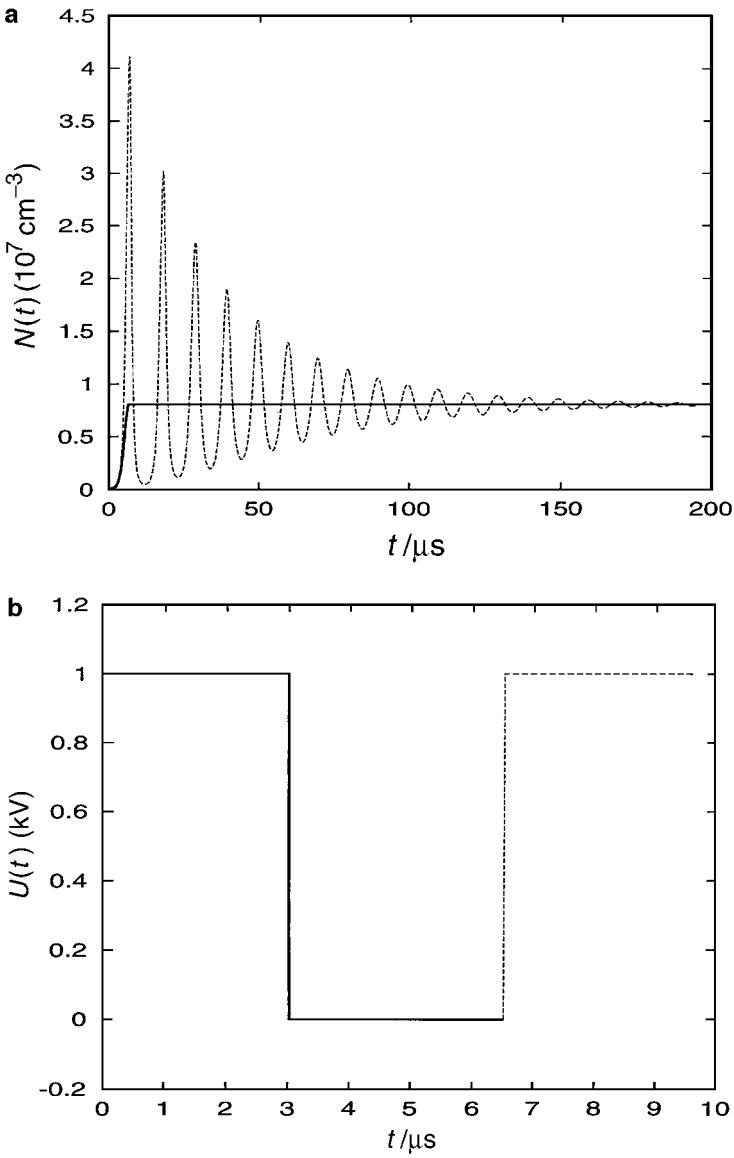

FIG. 6. $\tau_M = 10^{-4}$ s: (a) Carrier density $N(t)$ for $U(t) \equiv 1$ kV (dashed line) and for optimal control $U(t)$ (solid line). (b) Optimal control $U(t)$.

4. FURTHER CASES AND EXTENSIONS

In this section, we study how different bounds on the control variable and an additional bound on the electric field affect the optimal control solution. Section 4.3 relates the dynamic equations of the present paper to the general form of a two-dimensional Lotka–Volterra system considered in [12].

4.1. *Different Bounds on the Control Variable*

In (4) we have introduced the bounds $0 \le U(t) \le 1$ [kV] on the control variable. Instead of these bounds we may consider more general constraints,

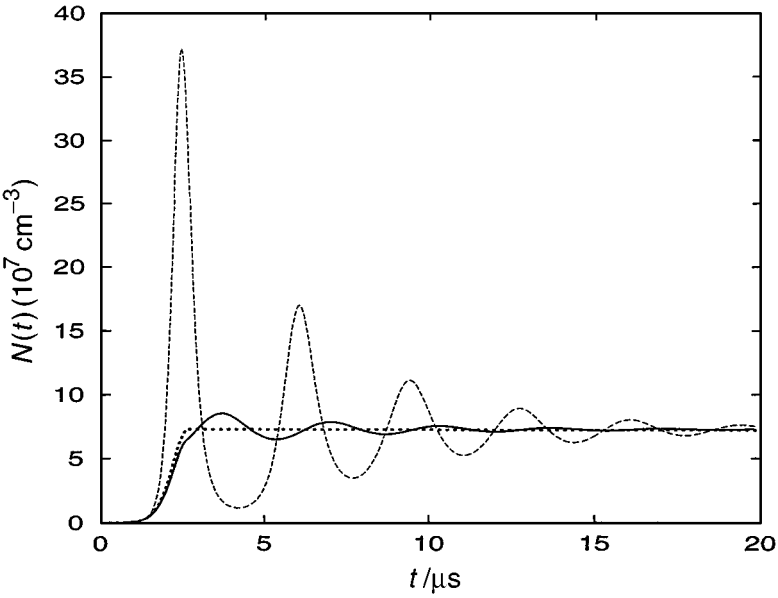

FIG. 7. Carrier density $N(t)$ for $\tau_M = 1.1 \times 10^{-5}$ s using different control strategies: $t_{10} = 16.2\ \mu$s: $U(t) \equiv 1$ kV (fine dashes); $t_f = 2.67\ \mu$s: optimal control (bold dashes); $t_{10} = 5.55\ \mu$s: using optimal control for $\tau_M = 1.0 \times 10^{-5}$ s (solid line).

$$0 \le U_{min} \le U(t) \le U_{max} \qquad \text{for } 0 \le t \le t_f, \quad U_{max} \ge 1\ [\mathrm{kV}]. \tag{21}$$

The minimization of the final time t_f subject to the terminal conditions (10) and the control constraints (21) leads again to an optimal bang–bang control with structure (19). Mathematically, it is clear that the effective transient time *decreases* if we choose the lower bound $U_{min} = 0$ and *increases* the upper bound $U_{max} > 1$ since the set of admissible control functions is enlarged. For the bounds $U_{min} = 0$ kV and $U_{max} = 2$ kV, we obtain the following results using the code BNDSCO in [22]:

$$\tau_M = 10^{-5}\ \mathrm{s}: \qquad t_1 = 0.55898711\ \mu\mathrm{s}, \quad t_f = 2.22075263\ \mu\mathrm{s},$$
$$\lambda_E(0) = -1.25192600 \times 10^{-10}, \quad \lambda_N(0) = -37.39775718 \times 10^{-13}.$$

Again, the precise values are only given to prove the accuracy of the numerical method. The corresponding optimal densities of carriers and control are shown in Fig. 8. The minimal transient time t_f is only a slight improvement over the one for $U_{max} = 1$ kV. For that reason, there is no need to introduce a higher bound for the control at the expense of a more difficult technical implementation.

4.2. *Upper Bound on the Electric Field*

Looking at the graph of the optimal electric field $E(t)$ in Fig. 4, one may further put a constraint on the electric field according to

$$E(t) \le E_{max} \qquad \text{for } 0 \le t \le t_f. \tag{22}$$

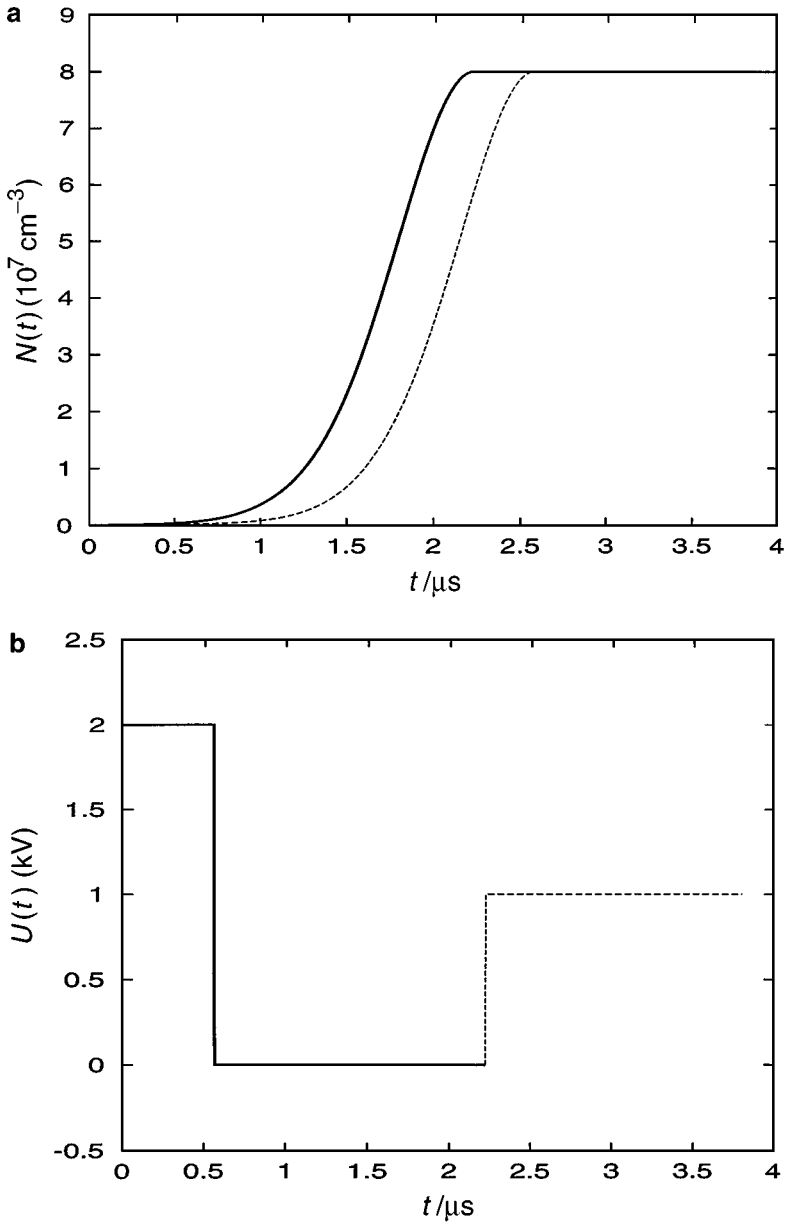

FIG. 8. $\tau_M = 10^{-5}$ s: (a) carrier density $N(t)$ for $U(t) \in [0, 1]$ [kV] (dashed line) and for $U(t) \in [0, 2]$ [kV] (solid line). (b) Optimal control $U(t) \in [0, 2]$ [kV].

The upper bound will become active if E_{max} is less than the maximal value of $E(t)$ in Fig. 4. The state constraint (22) is of *order* 1 since the first time derivative of $E(t)$ in (1) contains the control variable explicitly. For a survey on state-constrained control problems and the definition of the order of a state constraint, the reader may refer to Hartl *et al.* [4]. The typical situation for state constraints of order 1 is that the optimal solution contains a *boundary arc* characterized by

$$E(t) \equiv E_{max} \qquad \text{for } t_1^b \le t \le t_2^b, \quad 0 < t_1^b < t_2^b < t_f. \tag{23}$$

The points t_1^b and t_2^b are called *entry point* and *exit point* of the boundary arc, respectively. On a boundary arc we have the relation

$$0 = \frac{dE}{dt} = \left(\frac{U(t)/d - E(t)}{\tau_M} - bN(t)E(t) \right),$$

from which the following expression for the *boundary control* is obtained:

$$U(t) = U^b(t) := d(E(t) + \tau_M bN(t)E(t)) \qquad \text{for } t_1^b \le t \le t_2^b. \tag{24}$$

Under the additional constraint (22) the optimal control for minimal final time t_f has the structure

$$U(t) = \begin{cases} 1, & \text{if } 0 \le t \le t_1^b, \\ U^b(t), & \text{if } t_1^b \le t \le t_2^b, \\ 0, & \text{if } t_2^b \le t \le t_f. \end{cases} \tag{25}$$

Choosing the upper bound $E_{max} = 2.5 \times 10^4$ V/cm, we obtain the following optimal solution using the code BNDSCO in [22]:

$$\tau_M = 10^{-5}\text{s}: \qquad t_1^b = 0.64699091\ \mu\text{s}, \quad t_2^b = 2.63439313\ \mu\text{s}, \quad t_f = 3.16166836\ \mu\text{s},$$
$$\lambda_E(0) = -1.25192600 \times 10^{-10}, \quad \lambda_N(0) = -7.85683006 \times 10^{-13}.$$

The optimal control, respectively the optimal trajectories $N(t)$ and $E(t)$, are displayed in Figs. 9 and 10.

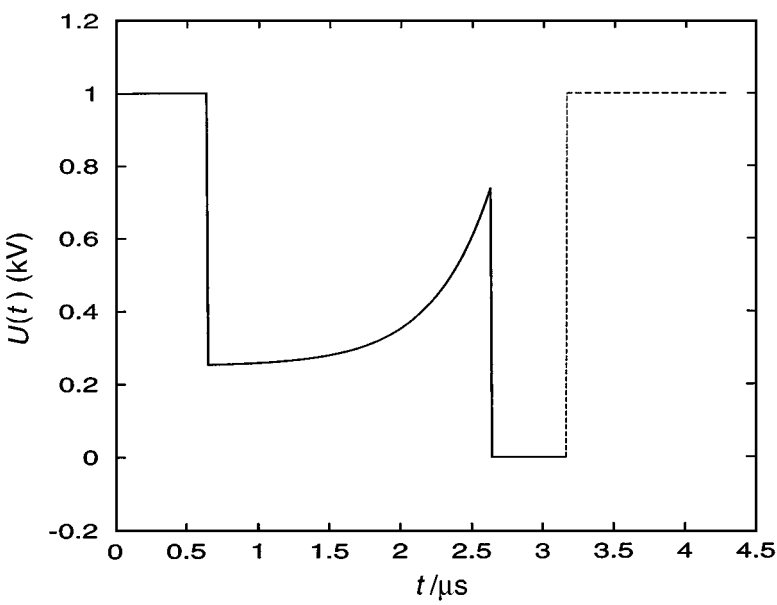

FIG. 9. $\tau_M = 10^{-5}$ s: optimal control $U(t) \in [0,\ 1]$ [kV] for the state constraint $E(t) \le E_{max} = 2.5 \times 10^4$ V/cm.

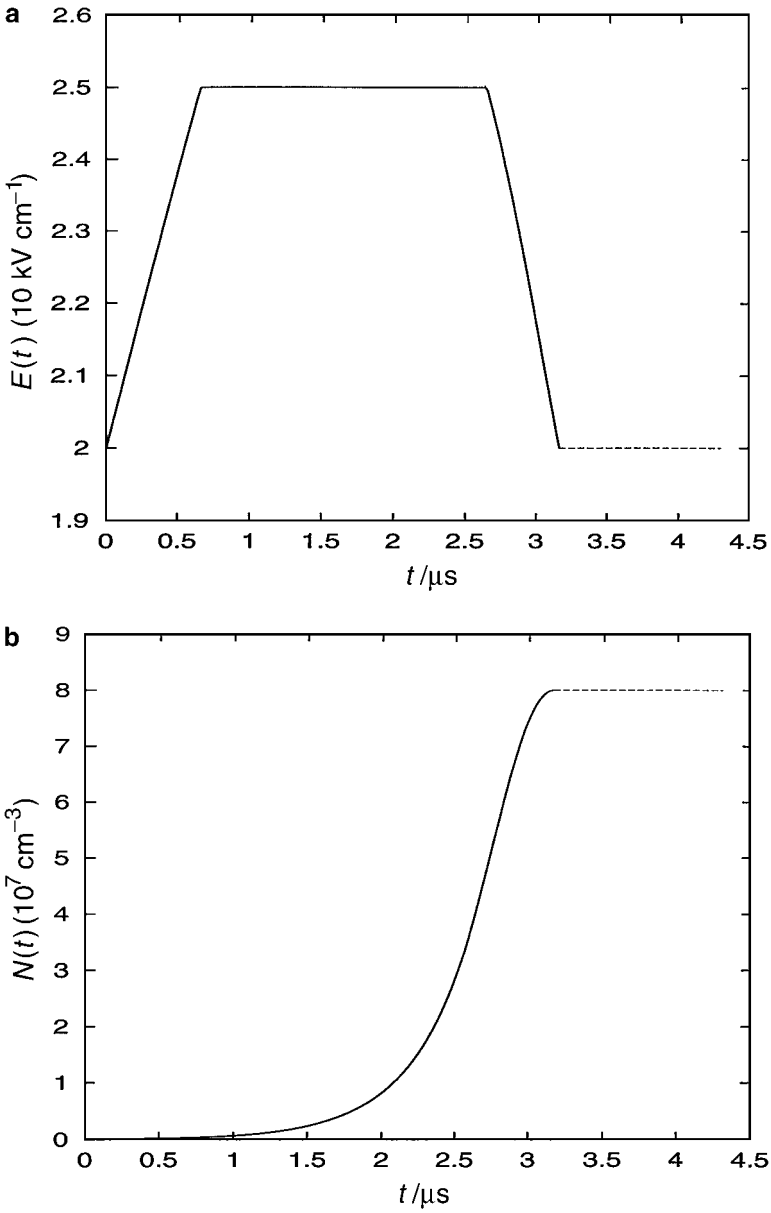

FIG. 10. $\tau_M = 10^{-5}$ s: optimal solution $E(t)$ and $N(t)$ for the state constraint $E(t) \le E_{max} = 2.5 \times 10^4$ V/cm.

4.3. *Time Optimal Control of a Lotka–Volterra System*

Lippi *et al.* [10–12] observed that, under appropriate scaling of state variables and time, their dynamical system can be transformed to the Lotka–Volterra system for two species x and y:

$$\dot{x} = -\varepsilon(x + xy - v), \quad \dot{y} = -y + xy, \quad \varepsilon > 0, \quad x(0) = x_0, \quad y(0) = y_0, \tag{26}$$

with given initial values x_0 and y_0. The derivative is taken with respect to a new time variable t, which is omitted for simplicity as argument on the right-hand side. The *control variable*

v satisfies the control constraint

$$0 \le v(t) \le v_{max} \qquad \text{for } 0 \le t \le t_f, \quad v_{max} > 0. \tag{27}$$

The control problem considered in the preceding section can be brought into this form by using the time transformation $t \to t/\tau_t$ and by scaling the state variables $E(t)$, $N(t)$ and the control variable $U(t)$ according to

$$x(t) := \frac{E(t)}{E_c}, \quad y(t) := \tau_M b N(t), \quad v(t) := \frac{U(t)}{E_c d}.$$

The constant ε and the initial values in (26) then become $\varepsilon := \tau_r/\tau_M$, $x(0) = 1$, $y(0) = 4\tau_t/(\varepsilon\tau_M^0)$. The upper bound for the new control variable v is related to that for the old control variable U by $v_{max} := U_{max}/(E_c d)$. For $v(t) \equiv v_{max}$ a stationary point of the system (26) is

$$(x_s, y_s) := (1, v_{max} - 1).$$

This stationary point is asymptotically stable for $v_{max} > 1$, which is valid for $U_{max} = 1$ kV. The optimal control $v(t)$ which minimizes the final transient time t_f to reach the stationary point

$$x(t_f) = 1, \quad y(t_f) = v_{max} - 1,$$

is a bang–bang control where again the singular case in a control law similar to (18) can be excluded. In this way we are able to apply the optimal control methods of the present paper to the situation of lasers and may thus eventually improve the control strategies proposed in [10–12]. Numerical results will be reported in a future paper.

5. CONCLUSION

In [15, 16] the complicated physical processes occurring in a semiconductor discharge gap image converter were analyzed. There, the reduced mathematical model that was developed was based on the nonlinear dynamical equations (1) and (2) that contain only two state variables. We think, however, that this model correctly encounters, at least qualitatively, the main physical processes that occur in the device. These are the nonlinear autocatalytic process of multiplication of charge carriers (this process is of pseudo-inductive nature; that is, it proceeds with a time lag in response to a variation of the electric field amplitude in the gas discharge domain) and capacitive and resistive processes.

The behavior of the system using a *constant* feeding voltage was studied in [15, 16]. In this paper the feeding voltage has been considered as a *time-dependent control* function which can be adjusted to a desired purpose. An important practical issue is to determine a control function that minimizes the transfer time between two steady states of the system. To achieve this goal, we have used *optimal control theory* in a systematic way to compute optimal control functions for a variety of parameters and different constraints on control and state variables. Essentially, the optimal control is of *bang–bang type* with only two bang–bang arcs. The second bang–bang arc of the control has the effect that the transient transfer time is drastically reduced compared to a constant feeding voltage. Moreover, the

minimized transfer time has the important side effect that oscillations and overshooting phenomena in reaching a final high current state are totally suppressed.

We stress the importance of *nonlinear* processes in the system which provide the possibility of benefitting from the efficient optimal control strategies developed in the present work. To further illustrate this point, let us come back to quantitative data of the present analysis, e.g., to the results presented in Fig. 6. There, uncontrolled and controlled kinetics of the transition to an increased current state are compared. One can see that the introduction of the optimal control reduces the effective transition time (evaluated as the time needed to reach a final state within 10% of accuracy) from approximately 130 to 6 μs. It is instructive to evaluate the corresponding transient time of a hypothetical *linear* system that would have resistive and capacitive properties similar to those of the one considered in the present study.

For a *linear* system, the duration of the transient process can be evaluated by calculating its RC product, where R is the system's resistance and C the capacity. Again, as in Section 2, we use the same set of system parameters as in [15]. For the characteristic time $\tau_M = 10^{-4}$ s adopted in the calculation of data in Fig. 6, we would obtain the final current density on the order of 200 μA/cm^2. Because the amplitude of the feeding voltage is 1 kV, this corresponds to a resistance of 5×10^6 Ω cm^2. Because the typical capacity of the planar structure under investigation is 5×10^{-12} F/cm^2 (cf. [15]), we would find the RC product of about 25 μs. To reach a final state within the accuracy of 10%, one would need to wait for at least two time intervals of length RC.

We see that, in our example of a hypothetical *linear* system, the duration of the transient is on the order of 50 μs, which considerably exceeds the duration of the optimal control solution for the *nonlinear* system. We also point out that, to apply experimentally the theoretical findings of the present study, one needs a high-voltage source whose output amplitude can be varied in time according to the bang–bang strategies of Sections 3 and 4. As far as we know, today's experimental techniques (in the first place, based on the application of high-voltage MOSFET transistors) can meet these requirements.

As an application of the results of the present research, one can consider the fast conversion of a *spatially homogeneous* optical field from an IR domain to the visible or the near UV range. Here, the output field is also spatially homogeneous. In this application, the steering voltage has to be synchronized with respect to the incoming IR optical field. Currently, we are investigating the technical implementation of this requirement. It is evident that one needs an additional detector for the IR, which is used to determine the arrival time of the IR radiation. Moreover, some electronic scheme would have to trigger the source of the feeding voltage, which would then generate the pulse for the optimal bang–bang voltage. Evidently, the requirement for such a strict synchronization may be not necessary if the considered device is used as a pulse gas discharge lamp.

Let us mention that analogously to the control approach in [10–12] we also have dealt with a zero-dimensional system. In other words, we are only concerned with the integral value of an output variable whereas the spatial structure of the two-dimensional object is not taken into consideration. It is of further interest to study the optimization procedure in model situations where the optical field that excites the semiconductor electrode (and, in this way, determines the spatial field of τ_m) is *spatially nonhomogeneous* and may be modeled by some simple partial differential equations of parabolic type.

The results obtained seem to be applicable not only to the image converter structure but also to some other gas discharge technical devices whose dynamics can be described adequately by Eqs. (1) and (2). Finally, the findings of the work may be of practical importance

in application to other nonlinear electronic devices that work in a high-speed mode, e.g., to semiconductor switches.

ACKNOWLEDGMENTS

We gratefully acknowledge the support of the Deutsche Forschungsgemeinschaft. J.-H. R. Kim was supported by a scholarship of the Graduiertenkolleg "Nichtlineare kontinuierliche Systeme" of the Deutsche Forschungsgemeinschaft at the Westfälische Wilhelms-Universität Münster. We thank Dr. L. Portsel, who helped to obtain the experimental data presented in Fig. 2. We also thank Professor Gian Luca Lippi for an enlightening discussion on lasers and an anonymous reviewer for helpful comments.

REFERENCES

1. L. S. Pontryagin, V. G. Boltyanskii, R. V. Gamkrelidze, and E. F. Miscĕnko, *The Mathematical Theory of Optimal Processes* (Fizmatgiz, Moscow, 1961; English translation: Pergamon Press, New York, 1961).
2. M. Hestenes, *Calculus of Variations and Optimal Control Theory* (John Wiley, New York, 1966).
3. A. E. Bryson and Y. C. Ho, *Applied Optimal Control*, Revised Printing (Hemisphere, New York, 1975).
4. R. F. Hartl, S. P. Sethi, and R. G. Vickson, A survey of the maximum principles for optimal control problems with state constraints, *SIAM Rev.* **37**, 181 (1995).
5. H. J. Pesch, A practical guide to the solution of real-life optimal control problems, *Control Cybernet.* **23**, 7 (1994).
6. J. T. Betts, Survey of numerical methos for trajectory optimization, *J. Guidance Control Dyn.* **21**, 193 (1998).
7. H. Haken, *Synergetics* (Springer-Verlag, Berlin, 1978).
8. E. Schoell, *Nonequilibrium Phase Transitions in Semiconductors—Self-Organization Induced by Generation and Recombination Processes* (Springer-Verlag, Berlin, 1987).
9. A. V. Gorbatyuk and P. B. Rodin, Current filaments in bistable semiconductors systems with two global constraints, *Z. Phys. B: Condensed Matter* **104**, 45 (1997).
10. G. L. Lippi, P. A. Porta, L. M. Hoffer, and H. Grassi, Control of transients in "lethargic" systems, *Phys. Rev. E* **59**, R32 (1999).
11. G. L. Lippi, S. Barland, N. Dokhane, F. Monsieur, P. A. Porta, H. Grassi, and L. M. Hofer, Phase space techniques for steering laser transients, *J. Opt. B: Quantum Semiclass. Opt.* **2**, 1 (2000).
12. G. L. Lippi, S. Barland, and F. Monsieur, Invariant integral and the transition to steady states in separable dynamical systems, *Phys. Rev. Lett.* **85**, 62 (2000).
13. K. H. Schoenbach, A. El-Habachi, M. M. Moselhy, W. H. Shi, and R. H. Stark, Microhollow cathode discharge excimer lamps. *Phys. Plasmas* **7**, Part 2, 2186 (2000).
14. F. Sauli, GEM: A new concept for electron multiplication in gas detectors, *Nucl. Instr. Meth. A* **386**(2–3), 531 (1997).
15. Yu. A. Astrov, L. M. Portsel, S. P. Teperick, H. Willebrand, and H.-G. Purwins, Speed properties of a semiconductor–discharge gap IR image converter studied with a streak camera system, *J. Appl. Phys.* **74**(4), 2159 (1993).
16. Yu. A. Astrov, *Dynamic Properties of Discharge Glow in a Device with Resistive Electrode*, A. F. Ioffe Physico-Technical Institute Report No. 1255, 1988 (in Russian).
17. Y. P. Raizer, *Gas Discharge Physics* (Springer-Verlag, Berlin, 1991).
18. L. M. Portsel, Yu. A. Astrov, I. Reimann, E. Ammelt, and H.-G. Purwins, High speed conversion of infrared images with a planar gas discharge system, *J. Appl. Phys.* **85**, 3960 (1999).
19. P. Glansdorff and I. Prigogine, *Thermodynamic Theory of Structure, Stability and Fluctuations* (Wiley, New York, 1971).
20. Ch. Büskens, *Optimierungsmethoden und Sensitivitätsanalyse für Optimale Steuerprozesse mit Steuer- und Zustandsbeschränkungen*, Dissertation (Institut für Numerische Mathematik der Universität Münster, Münster, Germany, 1998).

21. Ch. Büskens and H. Maurer, SQP-methods for solving optimal control problems with control and state constraints: Adjoint variables, sensitivity analysis and real-time control, in *SQP-Based Direct Discretization Methods for Practical Optimal Control Problems*, edited by V. Schulz, *J. Comput. Appl. Math.* **120**, 85 (2000).
22. H. J. Oberle and W. Grimm, BNDSCO—A Program for the Numerical Solution of Optimal Control Problems, Internal Report No. 515–89/22. Institute for Flight Systems Dynamics, DLK, Oberpfaffenhofen, Germany (1989).